Available online at www.sciencedirect.com
ScienceDirect
Pattern Recognition Letters 28 (2007) 1407–1414
Pattern Recognition Letters
www.elsevier.com/locate/patrec

Off-line signature verification using DTW

A. Piyush Shanker, A.N. Rajagopalan *

Image Processing and Computer Vision Lab, Department of Electrical Engineering, Indian Institute of Technology Madras, Chennai, Tamil Nadu 600036, India

Received 14 July 2004; received in revised form 18 December 2006
Available online 2 March 2007

Communicated by T. Breuel

Abstract

In this paper, we propose a signature verification system based on Dynamic Time Warping (DTW). The method works by extracting the vertical projection feature from signature images and by comparing reference and probe feature templates using elastic matching. Modifications are made to the basic DTW algorithm to account for the stability of the various components of a signature. The basic DTW and the modified DTW methods are tested on a signature database of 100 people. The modified DTW algorithm, which incorporates stability, has an equal-error-rate of only 2% in comparison to 29% for the basic DTW method.

Keywords: Dynamic time warping; Signature verification; Stability of signatures

1. Introduction

Signatures form a special class of handwriting in which letters or words may not be clearly legible. Signatures often incorporate complex geometrical patterns that make them a relatively secure means for authentication, attestation and authorization in legal, banking, and other high security environments. The signature verification problem pertains to determining whether a particular signature is verily written by the same person as is claimed and whether forgeries can be determined. The shape of a signature remains relatively the same over time when it is written down on an established frame like a bank document. The main difficulty in the description of pertinent features lies in the local variability of the writing trace of the signature which varies from person to person.

There are on-line as well as off-line techniques for signature verification. In this paper, we focus on the off-line approach. Various off-line techniques have been proposed in the literature for the signature verification problem. These include techniques based on hidden Markov Models (Justino et al., 2000), directional pdf (Drouhard et al., 1996), stroke extraction (Lau et al., 2002), synthetic discriminant functions (Wilkinson et al., 1991), granulometric size distributions (Sabourin et al., 1997), neural classifiers (Bajaj and Choudhary, 1997; Huang and Yan, 1997), wavelets (Ramesh and Murthy, 1999), grid features (Qi and Hunt, 1994), elastic matching (Bruyne and Forre, 1986), and Dynamic Time Warping (DTW) (Herbst and Coetzer, 1998; Yoshimura and Yoshimura, 1997). Signature verification by 2-D elastic matching within the regularization theory framework is described in (Mizukami et al., 2002).

We propose a new off-line signature verification method that uses DTW to match suitably derived 1-D features extracted from digitized images of signatures. Our method is different from that of Yoshimura and Yoshimura (1997) which uses DTW to segment the signature into a fixed number of components and computes a component-wise dissimilarity measure. We also suggest modifications to the DTW algorithm to account for the stability of various sections of a signature. The need to include stability was originally suggested by Dimauro et al. (2002) for the on-line signature verification problem. We have suitably adopted it for the

* Corresponding author. Tel.: +91 44 2257 4433; fax: +91 44 2257 0120.
E-mail address: raju@ee.iitm.ac.in (A.N. Rajagopalan).

0167-8655/$ - see front matter
doi:10.1016/j.patrec.2007.02.016

off-line method. This primarily involves assigning weights to various components of a signature depending on their stability. We quantify stability of a component by using the knowledge of the warping paths between signatures of the same person. These weights are then used to modify the cost function involved with the warping paths. We show that the performance of the verification system improves significantly with the incorporation of the stability factor.

This paper is organized as follows. Image pre-processing and extraction of 1-D features from signature images is discussed in Section 2. In Section 3, we describe our basic DTW algorithm for signature verification. This is followed by the modified DTW algorithm in Section 4. Experimental results are given in Section 5 while Section 6 concludes the paper.

2. Pre-processing and feature extraction

In this section, we discuss geometric image alignment and extraction of 1-D features from signature images. Since a standard signature database is not available in the public domain, we built our own database to test the effectiveness of our system. Our signature database comprises of 1431 signatures collected from 100 people. Each individual was asked to provide 10 samples of his/her signature for training. We collected 300 samples of casual forgeries (3 for every person in the database) and 75 genuine probe signatures for testing. We also collected a set of 56 skilled forgeries. Sample signature images for each of these categories are given in Fig. 1. The signatures were collected on A4 sheets with boxes of size 2 cm × 8 cm, big enough to accommodate large signatures. An HP Scanjet 4400C was used to scan and digitize the images. The images were scanned at 150 dpi resolution and stored in bitmap format.

The scanned images may not be properly aligned. Hence, they must be pre-processed to account for any changes in orientation. Geometric correction is a necessary step before template matching can be done using DTW. The effectiveness of two types of pre-processing methods was investigated – the Maximum Length Vertical Projection (MLVP) method and the Minimum Length Horizontal Projection (MLHP) method. Both methods involve rotating the signatures by an angle and making decisions based on the lengths of the projections.

Let "I_0" refer to the scanned image and "I_θ" refer to the image rotated by an angle "θ". For practical purposes, we assume that the maximum variation in θ is from $-30°$ to $30°$. All the images under discussion span from the highest to the lowest non-zero pixel and the left-most to the right-most non-zero pixel. All indices are with reference to the top-left corner of the image which is represented by $(1,1)$.

2.1. The MLVP method

The vertical projection of an image is defined as

$$v_\theta(j) = \sum_i I_\theta(i,j). \tag{1}$$

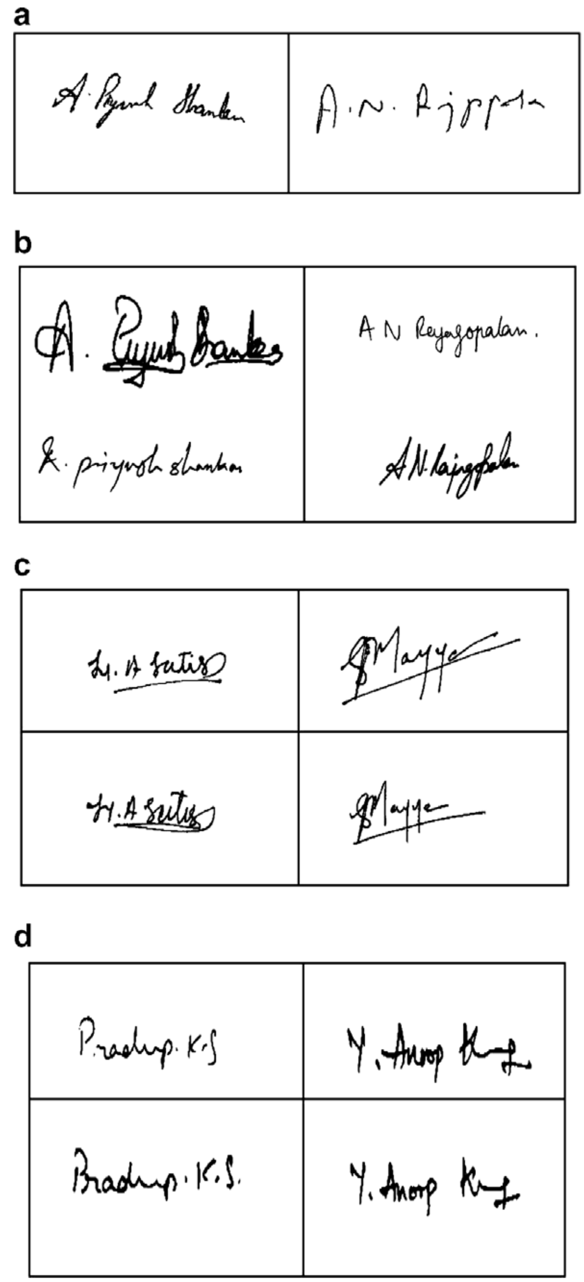

Fig. 1. Examples of (a) genuine signatures; (b) casual forgeries of signatures in (a); (c) skilled forgeries (top) of original signatures (bottom) and (d) genuine probe signatures (not used in training on top) along with images from training set (bottom).

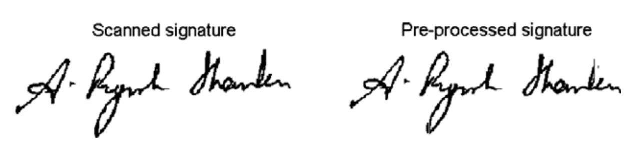

Fig. 2. The original signature (left) and its geometrically aligned version using MLVP (right).

We pick that "I_θ" as the reference template whose vertical projection has the maximum length. In Fig. 2, we show a signature before and after geometric alignment using

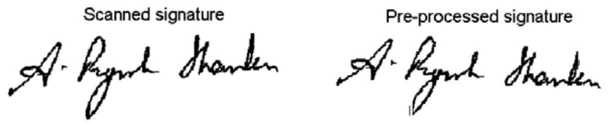

Fig. 3. The original signature (left) and its aligned version using MLHP (right).

MLVP. The image on the left is the original scanned signature and the image on the right shows the signature after alignment.

2.2. The MLHP method

The horizontal projection of an image is defined as

$$h_\theta(i) = \sum_j I_\theta(i,j). \tag{2}$$

From among these, we pick that "I_0" as the reference template whose horizontal projection is of minimum length. Fig. 3 shows an image that has been geometrically aligned using MLHP.

Both MLVP and MLHP perform satisfactorily for image alignment. We have chosen MLHP in the pre-processing stage of our method as its performance was found to be marginally better when used in conjunction with the modified DTW algorithm.

The 1-D features that are typically extracted for a signature image include vertical projection (VP), horizontal projection (HP), top contour, bottom contour, envelope width, and contour ratio (Bajaj and Choudhary, 1997). Among these, we selected VP as the primary 1-D feature to be used for verification. The vertical projection (v_θ) is the sum of pixels along the columns of a binary image. To make the feature sensitive to changes in scale, the signal is normalized by the square root of the length of the vertical projection. It is well-known that the vertical projection is a stable feature with good resolving power (Bajaj and Choudhary, 1997).

3. Dynamic time warping for signature verification

The Dynamic Time Warping (DTW) algorithm which is based on dynamic programming finds an optimal match between two sequences of feature vectors by allowing for stretching and compression of sections of the sequences. This feature of the algorithm makes it suitable for various speech recognition applications (Sakoe and Chiba, 1978).

For the signature verification problem, we extract the 1-D VP feature from the signature images. We pairwise match a reference template with a probe template by computing a measure of variation or dissimilarity between the two templates. The non-linear matching between the two 1-D templates is achieved on a rectangular grid as indicated in Fig. 4.

The two templates, '$\vec{a}$' of length 'I' extracted from the probe signature and '$\vec{r}$' of length 'J' extracted from the reference signature are aligned along the x-axis and the y-axis,

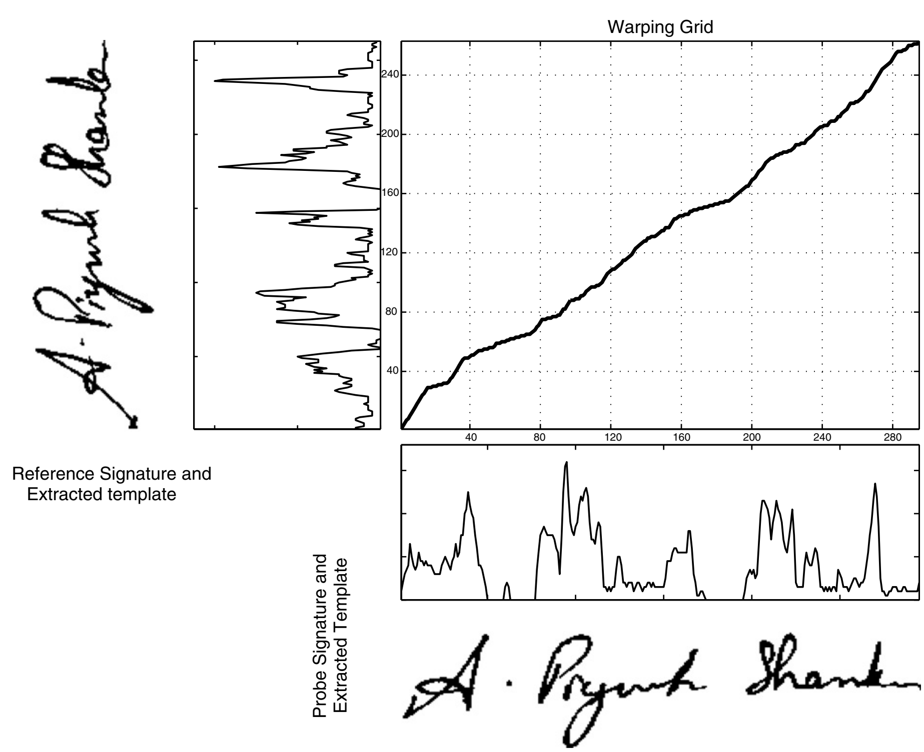

Fig. 4. The warping grid with the reference template and the probe template aligned along the y-axis and x-axis, respectively. The least cost path has been plotted. The signatures from which feature templates have been extracted are also shown.

respectively, as shown in Fig. 4. For convenience, we always use the shorter template along the y-axis. Each intersection on the grid is defined as a node (i,j) representing a match of the ith component of $\vec{a}$ with the jth component of $\vec{r}$. The cost matrix associated with the grid stores the value of the cost function associated with matching the ith component of $\vec{a}$ (extracted from the probe signature) with the jth component of $\vec{r}$ (extracted from the reference signature). Let the cost function be represented by $d_f(i,j)$. The cost at dummy node $(0,0)$ is defined as 'zero'. All the warping paths start from this dummy node and $d_f(0,0) = 0$.

We identify a path starting from $(0,0)$ to (I,J) such that the least cost is incurred while traversing the grid between the two points. This would provide us with a match with the least cost of variation or dissimilarity measure. We make a reasonable assumption that the starting and ending pixels of the two signatures being compared match. The cost thus computed can be used for comparison with similar costs computed using signatures in the training set.

A 'path' is defined as a concatenation of node pairs extending from (i_{k-1},j_{k-1}) to (i_k,j_k). The variables 'i_k' and 'j_k' indicate the indices of 1-D VP feature vectors $\vec{a}$ and $\vec{r}$ (extracted from the signatures) at instance 'k' of matching. A path starting from $(0,0)$ and ending at (i_k,j_k) has an overall cost associated with it. We use $D(i_k,j_k)$ to denote this type of cost, and it is defined as

$$D(i_k, j_k) = D(i_{k-1}, j_{k-1}) + d_f(i_k, j_k). \tag{3}$$

Since node $(0,0)$ is the dummy starting node for all paths, $D(0,0) = 0$.

By an iterative process, we find that

$$D(i_k, j_k) = \sum_{m=0}^{k} d_f(i_m, j_m). \tag{4}$$

The problem can be reduced to finding a sequence of nodes (i_k,j_k) which minimizes the accumulated cost for a complete path ending at node (I,J):

$$\begin{aligned} D^*(i_k, j_k) &= \min\left[D(i_{k-1}, j_{k-1})\right] + d_f(i_k, j_k) \\ &= \min\left[\sum_{m=0}^{k} d_f(i_m, j_m)\right]. \end{aligned} \tag{5}$$

For the final cost, we substitute in the equation $(i_K,j_K) = (I,J)$.

Using the above formulation, the matching problem can be reduced to finding the path corresponding to the least cost of variation or the least dissimilarity measure between vectors representing 1-D VP features extracted from the probe and reference signatures.

The dynamic programming algorithm as formulated above is computationally intensive and the process can be speeded up by using *a priori* information about the templates being matched. The paths in the search space can be considerably pruned by application of certain constraints. We discuss these constraints below.

3.1. End-point constraints

The starting point and the ending point of the warping path are fixed at $(0,0)$ and (I,J). We assume that the first and last set of non-zero pixels of the signatures to be compared match as shown in Fig. 5.

3.2. Continuity constraint

The continuity constraint ensures that there is no break in the path, i.e.,

$$i_k - i_{k-1} = 1. \tag{6}$$

In other words, matching is accomplished along the axis of the feature extracted from the probe signature. This constraint would also imply that 'K' in Eq. (5) is the same as 'I'.

3.3. Monotonicity constraint

The sequence of characters in a signature is constant. The monotonicity constraint requires the characters to be clustered in monotonically increasing order, which means

$$j_k - j_{k-1} \geqslant 0. \tag{7}$$

3.4. Global path constraint

This constraint is used to restrict the extent of compression or expansion of the features extracted from the signatures. The spatial variability can be considered to be limited which implies that we can prune the search space. We use a slope constraint to reduce the legal search region as indicated in Fig. 5. The slope parameter is a measure of the maximum allowable stretch or the compression. It is implemented as shown below:

$$\begin{aligned} \max J = \min(&\text{slop} * i - \text{slop} + 1, \text{slopinv} * i \\ &- \text{slopinv} * I + J), \end{aligned} \tag{8}$$

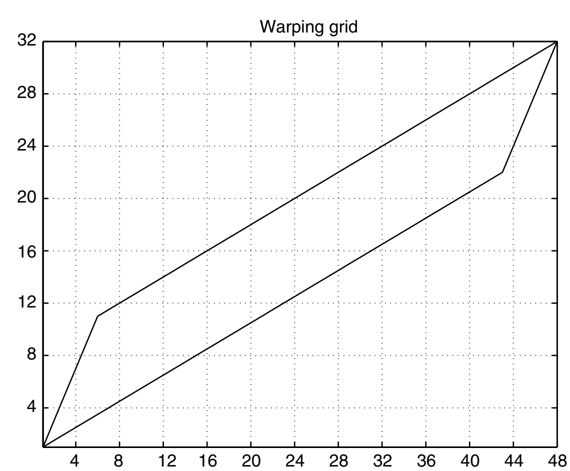

Fig. 5. Warping grid for $I = 48$ and $J = 32$. The feasible region is determined by the global path constraints as shown. The end-point constraints ensure that the points $(1,1)$ and (I,J) are part of the warping path.

$$\min J = \max(\text{slopinv} * i - \text{slopinv} + 1, \text{slop} * i - \text{slop} * I + J), \tag{9}$$

where 'slop' is the maximum allowed slope of the warping path, $\text{slopinv} = (\text{slop})^{-1}$, '$i$' is the index along the feature extracted from the probe signature, '$\max J$' and '$\min J$' represent the maximum and minimum permissible spatial indices of the legal search region at point 'i'.

We have used a simple distance function throughout for analysis, which is

$$d_f(i,j) = |a(i) - r(j)|. \tag{10}$$

The final warping cost $D(I,J)$ is normalized by the length of the feature extracted from the reference signature. This change enhances the resolution based on the warping cost. We have

$$\text{cost} = \frac{1}{J} * D(I,J). \tag{11}$$

4. Modified DTW algorithm

In automated signature verification, signature variability is a critical aspect which can affect verification performance. According to Dimauro et al. (2002), the basic task of reproducing a signature can be broken down in to several subtasks. Each subtask concerns the imitation of one segment of a signature and consists of three steps performed serially: perception, preparation and execution. Hence, the general format of difficulty in imitation of a signature is given by the difficulty in perceiving a spatial target and executing the subtask. Dimauro et al. (2002) proposed a new approach for on-line verification by quantifying the stability of various components of a signature and by making comparisons between the genuine signatures of a writer. The approach is based on the assumption that a highly stable component of a signature would be more difficult to reproduce than a highly variable component. Thus, local stability can be used to weight the strength of each part of a signature.

We propose a modification to the basic DTW algorithm described in Section 3 that incorporates a stability factor for better off-line signature verification.

Let $S = S^r | r = 1,2,\ldots,n$ be a set of 'n' templates of the same writer. By a template, we mean the same 1-D VP feature extracted from each of the writer's signatures. Each S^r can be described as:

$$S^r = (z^r(1), z^r(2), \ldots, z^r(M_r)). \tag{12}$$

Here '$z^r(i)$' denotes the value of the function representing the extracted 1-D feature at spatial index or position 'i'. The variable 'M_r' represents the length of the feature extracted from the signature 'S^r'.

Let S^r and S^t be two genuine signatures of the set ($S^r, S^t \in S$). A warping path 'W' between S^r and S^t is any sequence of couple of indices identifying points of S^r and S^t to be joined, i.e.,

$$W(S^r, S^t) = (i_1, j_1), (i_2, j_2), \ldots, (i_K, j_K), \tag{13}$$

where (k: i_k, $j_k \in N$, $1 \leqslant k \leqslant K$, $1 \leqslant i_k \leqslant M_r$, $1 \leqslant j_k \leqslant M_t$, $K = \max(M_r, M_t)$). If we consider a distance measure $d(i_k, j_k) = d_f(z^r(i_k), z^t(j_k))$ between points of S^r and S^t, we can associate to $W(S^r, S^t)$ a cost of variation or a dissimilarity measure (also refer to Eq. (4)):

$$D_{W(S^r,S^t)} = \sum_{k=1}^{K} d(i_k, j_k). \tag{14}$$

The matching procedure detects the warping path $W^*(S^r, S^t) = (i_1,j_1)^*, (i_2,j_2)^*, \ldots, (i_K,j_K)^*$ which satisfies the imposed constraint and results in

$$D_{W^*(S^r,S^t)} = \min_{W(S^r,S^t)} [D_{W(S^r,S^t)}]. \tag{15}$$

From $W^*(S^r, S^t)$ we identify Direct Matching Points (DMPs) of S^r with respect to S^t. A Direct Matching Point (DMP) of a signature S^r with respect to S^t is a point which has a one-to-one coupling with a point of S^t. In other words, let $z^r(p)$ be a point of S^r coupled with $z^t(q)$ of S^t; $z^r(p)$ is DMP of S^r with respect to S^t if and only if:

(1) $\forall \hat{p} = 1, \ldots, M_r$.
$\hat{p} \neq p \Rightarrow z^r(\hat{p})$ is not coupled with $z^t(q)$.
(2) $\forall \hat{q} = 1, \ldots, M_t$.
$\hat{q} \neq q \Rightarrow z^t(\hat{q})$ is not coupled with $z^r(p)$.

A DMP indicates the existence of a region of the rth signature which is roughly similar to the corresponding region of the tth signature. Therefore, for each point of S^r, a score is introduced according to its type of coupling with respect to the points of S^t, i.e.,

$$\forall p = 1,2,3,\ldots,M_r: \ \text{score}^t(z^r(p)) = \begin{cases} 1 & \text{if } z^r(p) \text{ is a DMP}, \\ 0 & \text{otherwise}. \end{cases} \tag{16}$$

The local stability function of S^r is defined as

$$\forall p = 1,2,\ldots,M^r : I(z^r(p)) = \frac{1}{n-1} \sum_{\substack{t=1 \\ t \neq r}}^{n} \text{score}^t(z^r(p)). \tag{17}$$

Please refer to Appendix A for an illustrative example of this idea.

Once the stability measure of the various components of the signature have been determined, this information needs to be incorporated into the computation of the 'Dissimilarity measure'. Let S^r refer to the feature extracted from the reference signature which is used to check the validity of the feature S^t extracted from the probe signature. Eq. (13) represents the match as computed using the Dynamic Time Warping algorithm. Eqs. (10) and (11) are still valid. We modify Eq. (14) to incorporate stability:

$$D_{W(S^r,S^t)} = \sum_{k=1}^{K} I(z^r(i_k)) d(i_k, j_k). \tag{18}$$

The modified score thus computed takes into account the stability of different sections of a person's signature and hence serves as a better measure of dissimilarity between two signatures than the one given by Eq. (14). Our results in Section 5 also support this claim.

4.1. Methodology for verification

In the training phase, the thresholds on the dissimilarity measures for each of the signatures are computed. The process of computing the thresholds can be broken down into the steps shown in Table 1.

Thresholds for every sample of all the writers are computed and stored for comparison with the probe signatures.

Table 1
Sequence of steps involved in computing the thresholds for the dissimilarity measure

1. $\forall i, j \leqslant N$ and $i \neq j$
Compute the warping path $W(S^i, S^j)$ between S^i and S^j
Here S^i and S^j are signature samples of the same writer
and 'N' samples are used for analysis of every writer
2. Compute the stability measure $I(z^i(p))$ using Eq. (17) for all i
3. Compute the dissimilarity measure $D_{W(S^i,S^j)}$ as given by Eq. (18)
4. Compute the threshold score
$\tau_i = \max(D_{W(S^i,S^j)}) \quad \forall i, j \leqslant N$

Table 2
Verification of the probe signatures

1. Compute $w_i = \frac{1}{\tau_i} D_{W(S^{pr},S^i)}$ for all $i \leqslant N$
2. Compute score $= \frac{1}{N}\sum_1^N w_i$
3. Make a decision based on the value of "score"

Let S^{pr} represent a probe signature. Analysis of the probe signature proceeds as shown in Table 2.

An example of analysis of a probe signature is given in Table 3. An averaging approach was adopted to compute the final 'score' as this would reduce the effect of any freak

Table 4
Effectiveness of the two verification systems in identifying casual forgeries, skilled forgeries and genuine signatures as a function of the threshold value

Hard threshold (m)	False acceptance (%) (casual forgeries)		False acceptance (%) (skilled forgeries)		True rejection (%) (non-training set)	
	DTW	Modified DTW	DTW	Modified DTW	DTW	Modified DTW
1.0	29.3	0.00	33.9	0.00	42.7	89.3
1.1	30.6	0.00	42.9	0.00	25.3	81.3
1.2	31.6	0.00	51.8	0.00	20.0	64.0
1.3	34.3	0.00	57.1	5.36	13.3	53.3
1.4	35.3	0.33	67.8	12.5	10.6	44.0
1.5	39.0	0.33	75.0	19.6	5.33	26.6
1.6	41.0	0.33	82.1	25.0	5.33	21.3
1.7	44.3	1.33	87.5	28.6	2.66	12.0
1.8	46.3	1.66	94.6	30.4	2.66	5.33
1.9	51.0	2.33	96.4	37.5	2.66	0.00
2.0	54.3	3.66	96.4	51.8	0.00	0.00
2.1	55.6	4.33	98.2	57.1	0.00	0.00
2.2	58.6	6.33	100	71.4	0.00	0.00
2.3	63.0	7.66	100	82.1	0.00	0.00
2.4	65.6	9.00	100	85.7	0.00	0.00
2.5	68.0	10.0	100	85.7	0.00	0.00

Table 3
Example of computation of dissimilarity score of a probe signature Pr_1

Img	I_1	I_2	I_3	I_4	I_5	I_6	I_7	I_8	I_9	I_{10}
Pr_1	0.071	0.065	0.083	0.078	0.082	0.075	0.090	0.085	0.079	0.091
Threshold	0.064	0.070	0.071	0.068	0.063	0.080	0.077	0.072	0.081	0.086
Ratio	1.109	0.929	1.169	1.147	1.302	0.938	1.169	1.181	0.975	1.058
Score	1.0977									

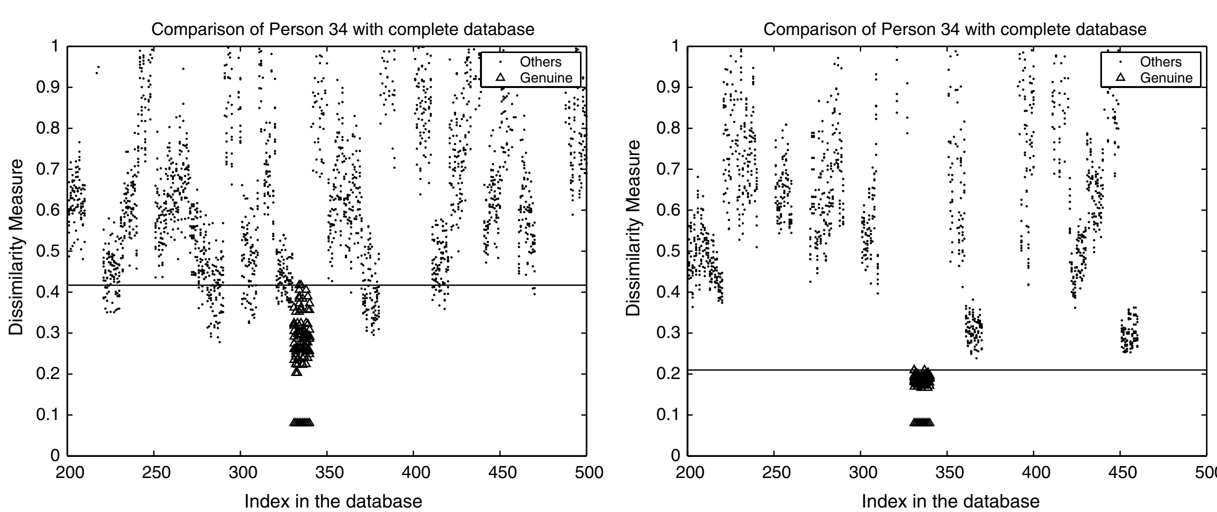

Fig. 6. Plot showing the resolving power of the vertical projection using the DTW (left) and modified DTW (right). Triangles indicate genuine signatures and dots signatures of other people. Threshold values for genuine signatures are also given.

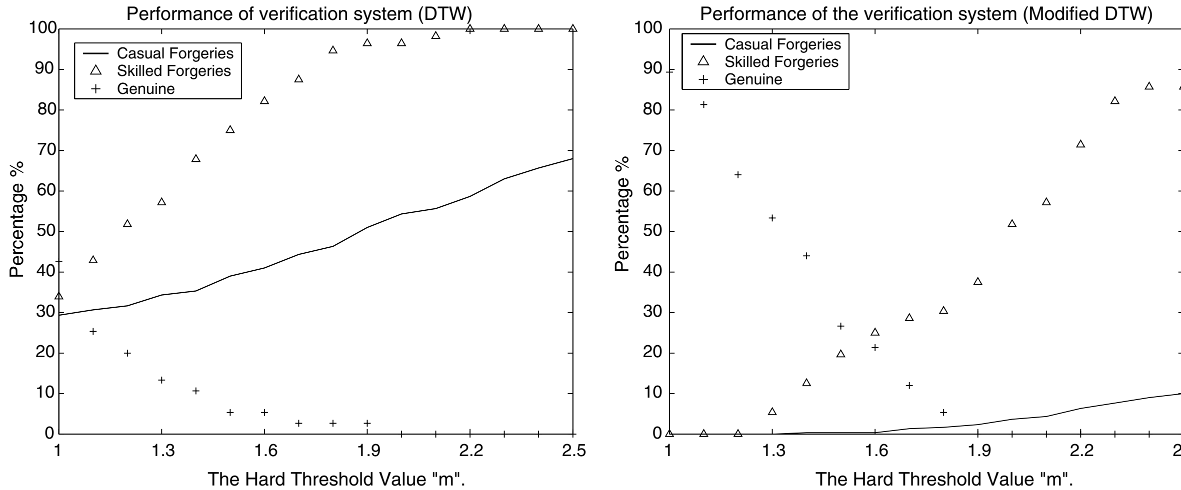

Fig. 7. Comparative plot showing the false acceptance percentage of casual as well as skilled forgeries and the true rejection percentage of genuine signatures as a function of m for the basic DTW (left) and modified DTW (right) methods.

instances of the vertical projections being similar to some of the training samples. This would require the probe signature to be consistently similar to the training templates to qualify as a "genuine signature".

A simple hard thresholding scheme with a threshold value, say 'm', was adopted and all probe signatures with scores more than this value were classified as "forgeries".

5. Experimental results

The 1-D VP feature was analyzed using both the DTW and the Modified DTW algorithms. An example of the effectiveness of the 1-D VP feature is shown in Fig. 6 for both the algorithms. From the figure, we note that the modified DTW performs much better than the basic DTW. It is able to better separate other signatures from the genuine ones.

All three types of probe signatures – genuine signatures, casual forgeries and skilled forgeries were next used for analyzing the effectiveness of the system. A simple hard-thresholding mechanism for decision-making was used as described in Section 4.1. The choice of the threshold value ("m") is critical for the performance of the system. The relative false acceptance and true rejection rates for casual forgeries, skilled forgeries and genuine signatures (not in the training set) for different values of the threshold value ("m") are listed in Table 4. Fig. 7 shows the comparison graphically.

In Fig. 7, when m is much larger than 1, the false acceptance rate for skilled forgeries is higher compared to casual forgeries for both the algorithms, as expected. When m approaches 1, it becomes increasingly difficult even for skilled forgeries to get through the system. Hence, as m is decreased to 1 the false acceptance curves corresponding to casual and skilled forgeries merge. From the plots, it is clear that the performance of the modified DTW is superior to the basic DTW method. Considering the plot for modified DTW in Fig. 7, we find that with a threshold value of 1.88, the system is able to distinguish casual forgeries and genuine signatures with an error rate of about 2%. The corresponding skilled forgery detection accuracy is about 65%. However, since the cost associated with a false acceptance is much more than a true rejection, the threshold value for a practical system would have to be smaller. It can also be observed that around a threshold value of 1.5, the system has close to 0% acceptance rate for casual forgeries, 20% acceptance rate for skilled forgeries, and about 25% rejection rate for genuine signatures.

6. Conclusions

An off-line handwritten signature verification system was proposed that uses the 1-D vertical projection feature in conjunction with DTW. Modifications were made to the basic DTW algorithm to account for stability of various components of a signature. The system based on the modified DTW algorithm performed significantly better than the basic system. The method is computationally efficient and runs in real-time.

Acknowledgements

The authors wish to thank the reviewers for their thoughtful comments and suggestions.

Appendix A. Example of computing weights for the components of a signature

Let $S = S^1, S^2, S^3$ be a set of three signatures of the same writer. Fig. A.1 shows the result of the match between S^1 and S^2, and S^1 and S^3.

The local stability function for the points of S^1 obtained from Eqs. (16) and (17) are shown in Table A.1.

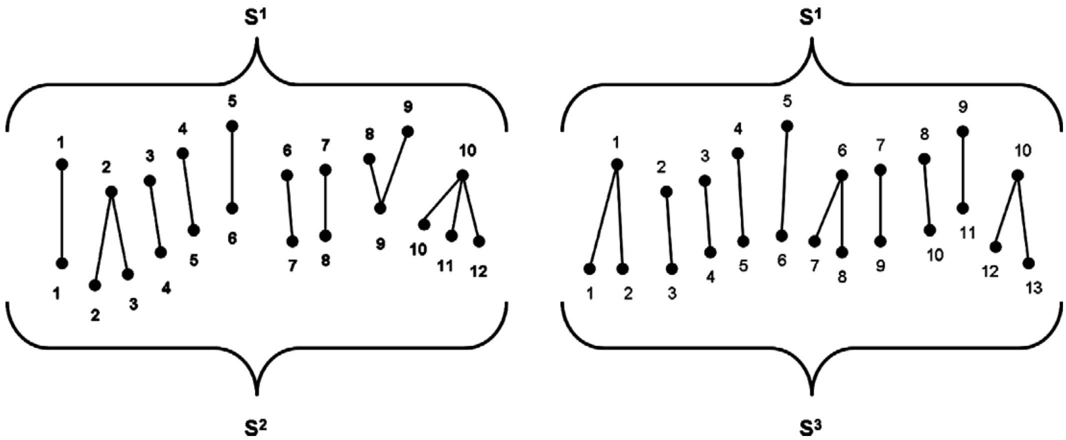

Fig. A.1. S^1 matches S^2 (left), and S^1 matches S^3 (right).

Table A.1
Local Stability values for S^1

Function\point	$z^1(1)$	$z^1(2)$	$z^1(3)$	$z^1(4)$	$z^1(5)$	$z^1(6)$	$z^1(7)$	$z^1(8)$	$z^1(9)$	$z^1(10)$
$\text{Score}^1(z^1(p))$	1	0	1	1	1	1	1	0	0	0
$\text{Score}^2(z^1(p))$	0	1	1	1	1	0	1	1	1	0
$I(z^1(p))$	0.5	0.5	1	1	1	0.5	1	0.5	0.5	0
Stability	M	M	H	H	H	M	H	M	M	L

Here H, M and L indicate high, moderate and low stability components, respectively.

References

Bajaj, R., Choudhary, S., 1997. Signature verification using multiple neural classifiers. Pattern Recognit. 30 (1), 1–7.

Bruyne, P., Forre, R., 1986. Signature verification with elastic image matching. Internat. Conf. Security Technol. 1, 12–14.

Dimauro, G., Impedovo, S., Modugno, R., Pirlo, G., Sarcinella, L., 2002. Analysis of stability in hand-written signatures. Proc. Internat. Workshop on Frontiers in Handwriting Recognit. (IWFHR) 8, 259–263.

Drouhard, J.P., Sabourin, R., Godbout, M., 1996. A neural network approach to off-line signature verification using directional pdf. Pattern Recognit. 29 (3), 415–424.

Herbst, B., Coetzer, H., 1998. On an offline signature verification system. In: Proc. of 9th Annual South African Workshop on Pattern Recognit. pp. 39–43.

Huang, K., Yan, H., 1997. Off-line signature verification based on geometric feature extraction and neural network classification. Pattern Recognit. 30 (1), 9–17.

Justino, E.J.R., Yacoubi, A.E., Bortolozzi, F., Sabourin, R., 2000. An off-line signature verification system using HMM and graphometric features. Proc. of Internat. Conf. on Pattern Recognit. 2, 11–17.

Lau, K.K., Yuen, P.C., Tang, Y.Y., 2002. Stroke extraction and stroke sequence estimation on signatures. Proc. of Internat. Conf. on Pattern Recognition 3, 119–122.

Mizukami, Y., Yoshimura, M., Miike, H., Yoshimura, I., 2002. An offline signature verification system using an extracted displacement function. Pattern Recognit. Lett. 23, 1569–1577.

Qi, Y., Hunt, B.R., 1994. Signature verification using global and grid features. Pattern Recognit. 27, 1621–1629.

Ramesh, V.E., Murthy, M.N., 1999. Off-line signature verification using genetically optimized weighted features. Pattern Recognit. 32, 217–233.

Sabourin, R., Genest, G., Prêteux, F.J., 1997. Off-line signature verification by local granulometric size distributions. IEEE Trans. Pattern Anal. Machine Intell. 19 (9), 976–986.

Sakoe, H., Chiba, S., 1978. Dynamic programming algorithm optimization for spoken word recognition. IEEE Trans. Acoust. Speech Signal Process. 26 (1), 43–48.

Wilkinson, T.S., Pender, D.A., Goodman, J.W., 1991. Use of synthetic discriminant functions for hand-written signature verification. Appl. Opt. 30 (23), 3345–3353.

Yoshimura, M., Yoshimura, I., 1997. An application of the sequential dynamic programming matching method to off-line signature verification. Lecture Notes in Computer Science. In: Proc. of First Brazilian Symposium on Advances in Document Image Analysis 1339. pp. 299–310.